Stochastic geolithological reconstruction coupled with artificial neural networks approach for hydrogeological modeling

Claudia Cherubini, Fausta Musci, Nicola Pastore

Abstract—When simulating fluid flow and solute transport a more accurate modeling of the lithologic, geological and structural characters of an aquifer is of extreme importance in order to improve the reliability of the numerical simulations. On the other hand the information available for the setting up of a hydrogeological model is subjected to ambiguities due to not univocal interpretations or to uncertainties linked to the methodologies of measurement of the variables of interest. Therefore, hydrogeological characterization of heterogeneous aquifers, if carried out up to a high degree of detail, should not identify a univocal model but a set of "equifinal" solutions.

In the present paper the application of Artificial Neural Network approach coupled with a Nested Sequential Indicator simulation has allowed to obtain the distribution of hydrogeologic parameters that are not only conditioned by the in situ measured values but also by the soft information coming from geolithology. The results show a fairly good relationship between parameters such as Transmissivity and Storage coefficient and the geolithologic architecture of the examined aquifer

Keywords— geolithological characterization, lithotypes, Sequential Indicator Simulation, Artificial neural networks approach, hydrogeological modeling

I. Introduction

Groundwater circulation as well as contaminant propagation is strongly affected by some aquifer properties. In the majority of studies, the sensitivity parameter of groundwater flow and transport models has proved to be hydraulic conductivity that can provide preferential pathways for groundwater movement and porosity, that influences flow velocity and takes part in the dispersive and diffusive phenomena occurring in the aquifer [1].

Usually in classical hydrogeological modeling of aquifers hydraulic properties are represented by equivalent parameters that are not representative of the geolithological reality but fit the observed data by means of calibration processes.

This method can be acceptable for some parameters but has proved to be oversimplified for the previously examined parameters, being both of them strongly linked to the aquifer geolithologic architecture. This can lead to not accurate predictions in groundwater circulation and contaminant propagation.

A more accurate modeling of the lithologic, geological and structural characters of an aquifer is of extreme importance when simulating fluid flow and solute transport in order to improve the reliability of the numerical simulations.

The aim of the present paper is to set up a hydrogeological model of a heterogeneous aquifer by means of an integrated approach. This method combines the use of pixel method called Nested Sequential Simulation for aquifer stochastic geolithological characterization implemented in a previous study [2] and Artificial Neural Networks in order to find a relationship between the obtained reconstruction and the measured hydraulic parameters. In such context the investigations carried out in the study area have determined the Transmissivity and Storage coefficient of the aquifer, parameters linked respectively to hydraulic conductivity and porosity.

In this way it is possible to obtain a hydrogeological model that is conditioned not only the in situ measured values but also by the soft information coming from geolithology.

II. Geological Setting

The study area is located in the so called Apulian Foreland, created during the Apennines' orogenesis, which is constituted by a thick succession of carbonatic rocks of platform. It appears as a high relief zone of tectonic origin, defined "horst", extended in direction North- West- South-East, from which two opposite step faults branch off: one plunges towards the Adriatic while the other plunges towards the Apennine.

Transversal faults interrupt the continuity of the horst structure of the Apulian Foreland constituting the depression of the Apulian Tavoliere, between Gargano and Murge, and the Plane of Brindisi, between the Murge and the Serre Salentine. Specifically the area is located in the tectonic depression opened towards the Adriatic coast and the Plane of Brindisi. This stepped depression has been filled up by the deposits of the Cycle of the Bradanic Trough and by the terraced marine deposits [3].

Manuscript received April 25, 2009: Revised version received May, 2009.

Claudia Cherubini is with Dipartimento di Ingegneria Civile e Ambientale Politecnico di Bari Via Orabona 4, 70100 Bari, ITALY (phone: 0039356881198, fax: 00390805481878, e-mail claudia.cherubini@poliba.it).

Fausta Musci is with Dipartimento di Ingegneria Civile e Ambientale Politecnico di Bari Via Orabona 4, 70100 Bari, ITALY (e-mail: f.musci@poliba.it).

Nicola Pastore is with Dipartimento di Ingegneria Civile e Ambientale Politecnico di Bari Via Orabona 4, 70100 Bari, ITALY (e-mail: nicola.pastore.ing@gmail.com).

The most ancient formation is represented by the micritic limestones and dolomites that can be ascribed to the platform formation of the Altamura Limestone, referred to the upper Cretacic. This formation constitutes the basement of the Salento Peninsula and extends for thousands of meters in depth. The asset is generally tabular with weakly dipping layers in direction SSE and SE.

Transgressively on this formation are present the soils corresponding to the lower terms of the sedimentary cycle of the Bradanic Trough constituted by the calcarenitic and bioclastic calciruditic deposits of coastal environment recognized as Gravina Calcarenites (upper Pliocene- Lower Pleistocene).

In continuity of sedimentation are present banks of subapennine clays (Lower Pleistocene) constituted by silty clays, marly clays and sandy clays and of blue- gray color, subordinately yellowish, averagely fossiliferous with horizons or sandy lenses. The deposits are based in continuity of sedimentation on Gravina Calcarenites and locally, along transgressive surfaces, directly on the Mesozoic deposits of the Altamura Limestone.

In the upper part there is the presence of more markedly silty- clayey and silty –sandy levels. This formation constitutes the impermeable substrate that sustains the shallow aquifer of the plain of Brindisi. The spatial continuity of these clayey deposits is of difficult reconstruction due to the frequent variations in thickness and local heterotopies with the calcarenitic deposits.

Over this clayey formation the Terraced Marine Deposits (middle- upper Pleistocene) are detectable, constituted by alternation of yellowish quartzous sands and organogenic calcarenites locally at lithoid character, with local intercalations of conglomeratic layers. Locally are detectable intercalations of lenses of grayish silts with particular frequency in the lower portion in proximity to the contact with the underlying subapenninic clays. These deposits lie along surfaces of marine abrasion detectable in the clayey and calcarenitic deposits of the cycle of the Bradanic Trough as well as of the Mesozoic limestones. This unity represents the shallow aquifer sustained by the blue- gray clays.

Where the marine terraced deposits do not crop out, above are detectable continental alluvial and eluvio- colluvial deposits (Olocene), constituted by sands, silts and clays variously distributed among themselves. They crop out principally along the erosion rills and in the most depressed areas near the coast, partially coating the pleistocenic terraced deposits. These deposits are interested by frequent oxidation phenomena and locally contain lapideous fragments and carbonatic material. Locally the continental deposits are of peaty type, indicating areas of deposit of marshy environment.

The geologic- structural lithologic characters give rise to two well distinct hydrogeological environments: the first shallow one, characterized by a phreatic groundwater contained in the terraced marine pleistocenic deposits and sustained by the pliopleistocenic clays. This aquifer, with modest discharge, is characterized by a local character and a maximum thickness of 37 m; the second, deep aquifer is represented by a calcareous aquifer constituted by carbonatic cretaceous fissured and karstified rocks, as well as calcarenites located in continuity and above the cretaceous rocks. This groundwater is nourished both by the precipitations coming upstream of the examined area, where the carbonatic formation crops out, and by the subterranean downflow coming from the contiguous Murgia. This groundwater flows towards the coast with hydraulic gradients generally lower than 0.05%, with modest piezometric heads, even many kilometers far away from the coast.

III. Nested SIS algorithm

Sequential indicator simulation (SIS) is a pixel based simulation algorithm that builds a categorical image, pixel after pixel, by drawing local probability distributions from the categories [4].

The principle of SIS algorithm is simple; it consists in the simulation of the series of K indicator values sequentially one location after another, each simulation being made conditional to all prior indicator data and all previously simulated variables [5].

The SIS algorithm consists in the following steps:

1. Define a random path that visits each location of the domain once. In each location $\mathbf{u}$, retain a specified number of neighboring conditioning data including both original indicator data and previously simulated location values.
2. At each location $\mathbf{u}$ along the path, estimate the membership probabilities of $\mathbf{u}$ to each categorical variables: $p^*(\mathbf{u};o_k \mid n)$ where n is the number of neighboring conditioning data.
3. Obtain Monte-Carlo simulation of the Indicator value by drawing a uniform random number $p \in [0,1]$ and by verifying for each categorical variable K if $p \le \sum_{j=1}^{k} p^*(\mathbf{u};o_j \mid n)$. If the j^{th} condition is true then the location $\mathbf{u}$ is assigned to categorical variable o_j, if not proceed with the $j+1^{th}$ condition in an analogous manner.
4. Add the simulated indicator value of the location $\mathbf{u}$ to the data set.
5. Repeat the previous steps 2, 3 and 4.
6. When all location $\mathbf{u}$ have been simulated, the stochastic realization is obtained.

The estimation of the membership probabilities of $\mathbf{u}$ to each categorical variable is obtained by solving a simple kriging system with local varying prior mean:

$$p^*(\mathbf{u};o_l \mid n) = p(\mathbf{u}) + \sum_{\alpha=1}^{n} \lambda_\alpha(\mathbf{u}) \cdot \{I(u_\alpha;k) - p(u_\alpha)\}$$

Where $\lambda_\alpha(\mathbf{u})$ are the simple kriging weights, $I(u_\alpha;k)$ are the indicator data at locations $\mathbf{u}_\alpha$, $p(\mathbf{u})$ and $p(\mathbf{u}_\alpha)$ are the respectively prior local probabilities at locations $\mathbf{u}$ and $\mathbf{u}_\alpha$.

The SIS algorithm is not sufficient to fully characterize low-entropy complex structures. In order to overcome this difficulty a specific procedure, called nested simulation technique, is proposed with the purpose to achieve a full geological characterization of aquifer.

This procedure consists in consecutive simulations for each categorical variable set constrained on the result of the previous categorical variable set simulations. The constrains are obtained by introducing the attraction parameter $a(\mathbf{u})$ [6] which increases or decreases the prior local probability if the location $\mathbf{u}$ is near to the bound of the previously simulated categorical variables. The prior local probability is obtained from vertical marginal proportion curve whereas the attraction parameter from embedded transition probability matrix for vertically successive occurrence of the lithofacies characteristic of depositional systems.

IV. Artificial Neural Network and training

The Artificial Neural Networks ANN are computational tools inspired by biological nervous system. Recently they have been used in a wide range of geological such as well test analysis [7], log interpretation [8], lithofacies modeling, permeability and porosity modeling [9], [10], [11], [12] and run-off modeling [13]. ANN are composed by a set of nodes, called neurons, interconnected in a network.

The most commonly used architecture of network is called feed forward network as the datum devolves one way through the network from the input layer, to the one or more hidden layers and finally to the output layer. In each elementary neuron of the hidden layer the set of normalized input data are converted by a weighting factor:

$$y_j = \sum_{i=1}^{m} w_{ij} \cdot x_i + w_{0j} \quad \mathrm{j} = 1,\dots,\mathrm{n}$$

where m are the input node, n are the hidden node and w_{0j} are the possible bias for the hidden node j. This function represents the input for the a differentiable transfer function "*f*", such as sigmoid function, that affords the final output of the neuron. In analogous manner the output of network are represented as:

$$z_k = \sum_{i=1}^{n} w_{jk} \cdot f\left(\sum_{i=1}^{m} w_{ij} \cdot x_i + w_{0j} \right) + w_{0k} \quad \mathrm{j} = 1,\dots,\mathrm{n} \quad \mathrm{k} = 1,\dots,\mathrm{l}$$

where l are the output nodes [14].

Once weights and biases have been initialized, the network is ready for learning. Back-Propagation neural network BPNN is a supervised learning technique as input dataset and the corresponding target output dataset are used to train a network in order to approximate the relationships themselves. The BPNN learns through an iterative procedure: the weights and the biases are continuously adjusted as long as the performance function, described by the mean of sum square of the errors network, is minimal [15]. The numerical optimization techniques, such as Levenberg-Marquardt algorithm, can be used for faster training. In each iteration step of damped version of Levenberg-Marquardt algorithm the current weight vector $\mathbf{w}_k$ is updated by a new estimate:

$$\mathbf{w}_{k+1} = \mathbf{w}_k - \left[\mathbf{J}_k^T \mathbf{J}_k + \lambda_k \mathbf{I} \right]^{-1} \mathbf{J}_k^T \mathbf{e}_k$$

Where $\mathbf{J_k}$ is the Jacobian matrix of the network errors respect to the weights and biases $\mathbf{e_k}$ is the network vector error and λ_k is the damping factor adjusted for each iteration [16].

One of the biggest problems in training neural networks is the overfitting of the training data. This problem can be overcome by using Bayesian regularization approach that control model complexity [17].

Usually in the regularization the mentioned error function is modified with additional terms:

$$M = \beta \left[\frac{1}{2} \sum_{i=1}^{N} e_i^2 \right] + \alpha \left[\frac{1}{2} \sum_{i=1}^{n} w_j^2 \right]$$

These terms permit to find weight factors with low aptitude to overfit the training data. The optimal inference of parameter α and β can be obtained assuming that the targets and the weights and biases are defined through Gaussian distribution where the parameters are related with variances of these distributions:

$$P(D \mid \mathbf{w}, \beta, H) = \frac{1}{\left(2\pi\alpha^{-1}\right)^{\frac{N}{2}}} \exp\left(-\frac{\alpha}{2} \sum_{i=1}^{N} e_i^2 \right)$$

$$P(\mathbf{w} \mid \alpha, H) = \frac{1}{\left(2\pi\beta^{-1}\right)^{\frac{n}{2}}} \exp\left(-\frac{\beta}{2} \sum_{i=1}^{n} w_i^2 \right)$$

where H represent the architecture of the network. Applying Bayes' theorem [18]:

$$P(\alpha, \beta \mid D, H) = \frac{P(D \mid \alpha, \beta, H) P(\alpha, \beta \mid H)}{P(D \mid H)}$$

The factor $P(D \mid \alpha, \beta, H)$ is called the "evidence" of the parameters themselves. Theirs optimal values can be attempted by searching the maximum of log of the evidence:

$$\log P(D \mid \alpha, \beta, H) = -M(\mathbf{w}) - \frac{1}{2} \log \det\left(\frac{\mathbf{A}}{2\pi} \right) - \frac{N}{2} \log\left(\frac{2\pi}{\alpha} \right) + -\frac{n}{2} \log\left(\frac{2\pi}{\beta} \right)$$

where $\mathbf{A}$ is equivalent to the Hessian matrix of the $M(\mathbf{w})$.

Results

V. Identified and modeling lithofacies unit sequences

Starting from the stratigraphies of about 220 boreholes carried out in the study area (that extends for 6.5 km^2), the soils belonging to this domain, on the basis of their lithostratigraphic characteristics have been grouped into the following five principal lithologic unities reported from the top to the bottom, after a shallow layer of anthropic material:

1. Filling material. Has a medium thickness variable generally from 0 and 2.5 m with maximum thicknesses equal to 6 m from the ground level. It is constituted by elements of various grain sizes and locally fragments of concrete and bricks are detectable.

2. Alluvial and colluvial deposits (Olocene). Have an average thickness variable generally from 0.5 to 5 m from the ground level. They are constituted by layers of sand, silt, silty sands and sandy silts, clayey silts and silty clays; especially on the basal part they are rich in carbonatic concretions.

3. Terraced marine deposits (Middle – Upper Pleistocene). Characterized by intercalations of fractured and

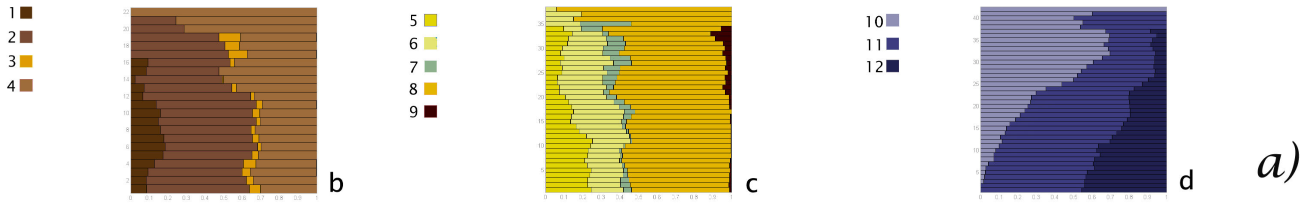

$$\begin{array}{c|cccc} & 1 & 2 & 3 & 4 \\ \hline 1 & - & 0.8400 & 0.0400 & 0.1200 \\ 2 & 0.1250 & - & 0.2143 & 0.6607 \\ 3 & 0.0625 & 0.3125 & - & 0.6250 \\ 4 & 0.0784 & 0.7255 & 0.1961 & - \end{array}$$

$$\begin{array}{c|ccccc} & 5 & 6 & 7 & 8 & 9 \\ \hline 5 & - & 0.2716 & 0.0864 & 0.5926 & 0.0494 \\ 6 & 0.3519 & - & 0.0185 & 0.5741 & 0.0556 \\ 7 & 0.2000 & 0.1667 & - & 0.5667 & 0.0667 \\ 8 & 0.4000 & 0.3889 & 0.1778 & - & 0.0333 \\ 9 & 0.3333 & 0.3333 & 0 & 0.3333 & - \end{array}$$

$$\begin{array}{c|ccc} & 10 & 11 & 12 \\ \hline 10 & - & 0.7547 & 0.2453 \\ 11 & 0.0833 & - & 0.9167 \\ 12 & 0 & 0 & - \end{array}$$

b)

	Model type	Azimuth	l_X [m]	l_Y [m]	l_{Zst}
1	*Exp*	0	200	200	0.22
2	*Exp*	0	200	200	0.22
3	*Exp*	0	225	225	0.14
4	*Exp*	0	200	200	0.23

	Model type	Azimuth	l_X [m]	l_Y [m]	l_{Zst}
5	*Exp*	15	425	275	0.10
6	*Exp*	0	180	180	0.33
7	*Exp*	0	110	110	0.14
8	*Exp*	0	200	200	0.36
9	*Exp*	0	350	350	0.10

	Model type	Azimuth	l_X [m]	l_Y [m]	l_{Zst}
10	*Sph*	0	180	180	0.26
11	*Sph*	0	175	175	0.26
12	*Sph*	0	230	230	0.26

c)

Fig. 1 *a)* Vertical facies proportions curves *b)* embedded transition matrixes *c)* spatial correlation structure. b = Alluvial and colluvial deposits, 1 = Silt, 2 = Sandy silt and silty sand, 3 = Sand, 4 = Clayey silt and silty clay, c = Terraced marine deposits (Middle – Upper Pleistocene), 5 = Calcarenitic levels, 6 = Sand, 7 = Sandy silt and silty sand, 8 = Sand with inclusions of calcarenite, 9 = Silt, clayey silt, silty clay and clay, d = Silty sands of the Middle Pleistocene, 10 = Sand, 11 = Silty sand and sandy silt, 12 Silt.

weathered calcarenitic levels and fine sand and at times silty sand or sandy silt; locally are present intercalations of lenses of clayey silts. These deposits host the shallow aquifer and have an average thickness of the order of 12-18 m from the ground level.

4. Silty sands of the Middle Pleistocene. Constituted by sands, sandy silts and silty sands of gray color. The silty fraction increases with depth together with the decrease of the sandy fraction. This deposit constitutes the top of the aquiclude.

5. Submarine blue – gray clays (Lower Pleistocene). Characterized essentially by gray clays that are detectable at depths higher than 26 m and constitute the aquiclude that sustains the shallow aquifer. This lithologic unity has not been characterized due to scarcity of information regarding it.

The horizon algorithm of GMS program is used to build three-dimensional models of lithofacies unit sequences. These algorithms honor borehole data and the manually cross-sections that define the interpreted structure of the litho sequences between boreholes (fig 1 a). This geological model represents the basis for the next stochastic simulations.

VI. Geostatistical simulation

To the model of the lithologic unit sequences is associated a three-dimensional grid constituted by (215×215×60) = 2.773.500 cells. In order to incorporate stratigraphic dips in the simulations the real vertical depth of the sample indicator data is transformed into a standardized depth through the following equation:

$$z_{st}^{j} = \left[z_{true}^{j} - z_{bot}^{j}\right] \cdot \left[z_{top} - z_{bot}\right]^{-1} \in [0,1]$$

Where z_{top} and z_{bot} are the depths of top and bottom of the grid, z_{st}^{j} is the standardized horizon, z_{true}^{j} is the true vertical depth, z_{bot}^{j} is the depth of the bottom of the j-th lithofacies unit sequence. Then geostatistical simulations are performed for each lithofacies unit in a regular standardized grid honoring the standardized indicator data, the vertical marginal probability, the embedded transition matrix, and the spatial correlation structure inferred from experimental variograms [2].

In the nested technique it is important to establish the order of the consecutive simulations of the lithotype set. Generally the principle is to order the lithotype from the highest entropy one to the lowest.

The simulation results obtained on the regular grid are smoothed using the GSLIB program "trans" (fig 2b) and are joined in the previous three-dimensional grid through the back-transformation of the standardized vertical depth into the true vertical depth. The final result is shown in fig. 2 c.

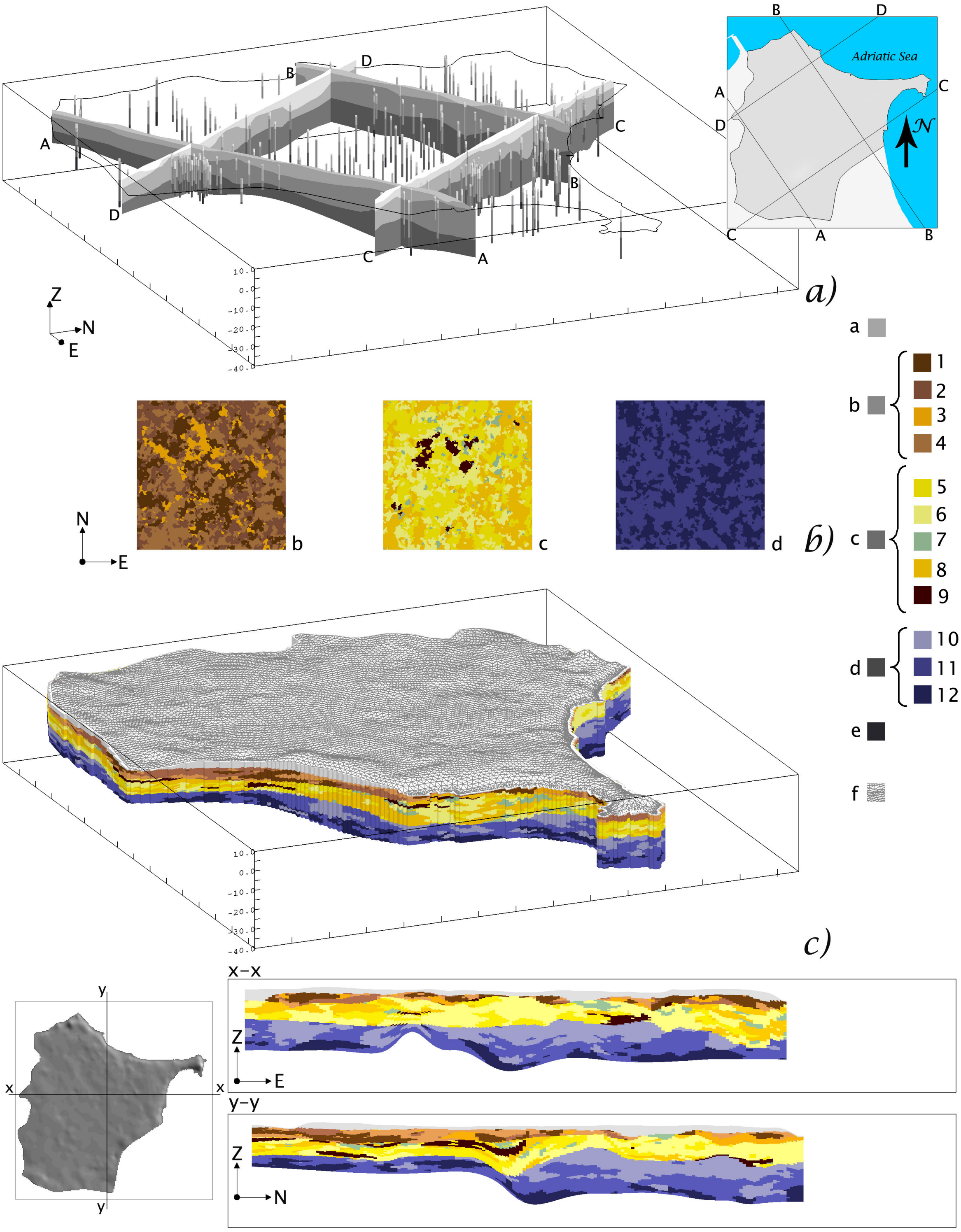

Fig. 2: a) three-dimensional models of lithofacies unit sequences b) geostatistical simulation results on the regular grid c) final result. Legend: a = Filling material, b = Alluvial and colluvial deposits, 1 = Silt, 2 = Sandy silt and silty sand, 3 = Sand, 4 = Clayey silt and silty clay, c = Terraced marine deposits (Middle – Upper Pleistocene), 5 = Calcarenitic levels, 6 = Sand, 7 = Sandy silt and silty sand, 8 = Sand with inclusions of calcarenite, 9 = Silt, clayey silt, silty clay and clay, d = Silty sands of the Middle Pleistocene, 10 = Sand, 11 = Silty sand and sandy silt, 12 Silt, e = Submarine blue – gray clays (Lower Pleistocene).

VII. WELL TEST ANALYSIS

The carried out investigations consist in recovery tests executed in piezometers located in the study area, characterized by constant withdrawals, (variable from piezometer to piezometer) and test duration variable from 1 to 2 hours, depending on the point of withdrawal. The data obtained from the tests are the values of residual drawdown, s', as a function of time, measured at the end of the pumping.

In the study area the aquifer behavior has been detected as confined in some zones and phreatic in others.

Therefore, in order to determine the hydrogeologic characteristics of the aquifer (Transmissivity, Storage coefficient) the two different aquifer behaviors have been assumed and for both of them the T and S values have been determined in correspondence of which the curves have best fitted the experimental data.

For this aim an algorithm of optimization has been implemented based on simulated annealing with two different objective functions, the former that makes the assumption of artesian aquifer and the latter that considers the aquifer as phreatic.

The first objective function is represented by the difference between experimental data and the theoretic curve, obtained from the following equation:

$$s' = Q \cdot Z(r, \tau + t) - Q \cdot Z(r, t)$$

In the second case, the objective function has been obtained by means of the equation:

$$H_0^2 - H^2 = Q \cdot Z'(r, \tau + t) - Q \cdot Z'(r, t)$$

With a corrective contribution on the storage coefficient, in order to take into account the reduction in aquifer saturated thickness; the corrected value S* is obtained by means of the following formulas [19]:

$$s^* = \frac{H_0}{H_0 - s} \cdot S$$

Where S is effective porosity and s mean drawdown in the considered point.

The transmissivity (T) and storage coefficient (S) values have been calculated by means of the algorithm with the objective function 1 and 2.

For each piezometer a graph has been realized, in which the experimental data and the theoretic curve are represented. By means of the diagrams it has been possible to evaluate if the theoretic curve approximates the mentioned data, once fixed an error range equal to the standard deviation of the theoretic curve (error bars). From the comparison of the values of the aquifer hydrogeologic parameters, calculated with the Theis recover function and with the algorithm that uses the objective function 1 and 2, it has been possible to ascertain that the obtained results have the same magnitude order.

In the subsequent analyses the data obtained by means of the algorithm have been used, rather than the ones determined by means of the Theis recovery function, because this formula allows to estimate just transmissivity.

From the analysis carried out on graphs, obtained from the minimization algorithm it has been possible to select the T and S values in correspondence of which the curves have best fitted the experimental data.

The algorithm that make use of the objective function 1 have proved to be the most representative of the effective aquifer behavior, except in some piezometers for which the theoretic curve of the objective function 2 best approximates the experimental data.

The T and S values in correspondence of four piezometers have been discarded because the theoretic curve, for both objective functions, does not approximate the experimental data. This exclusion can be attributable to the theoretic curve that is not adapt to fit the data or to the data themselves that can be affected by errors. In figure 3 and 4 are reported the histograms of the obtained T and S values.

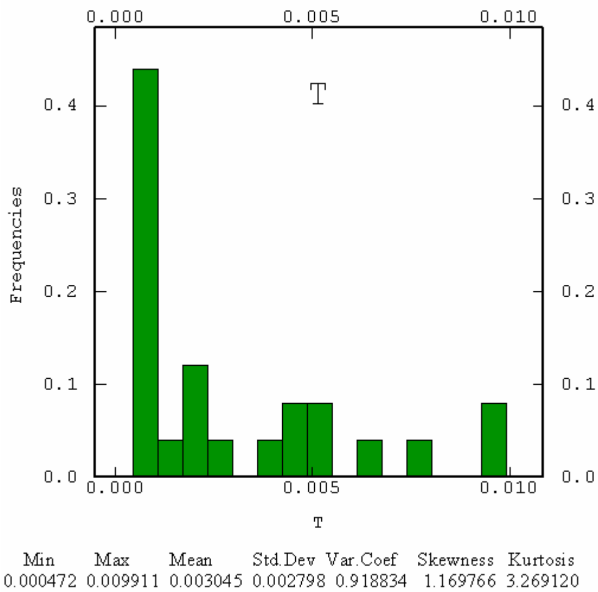

Fig. 3 Histogram of Transmissivity [$m^2 \cdot s^{-1}$]

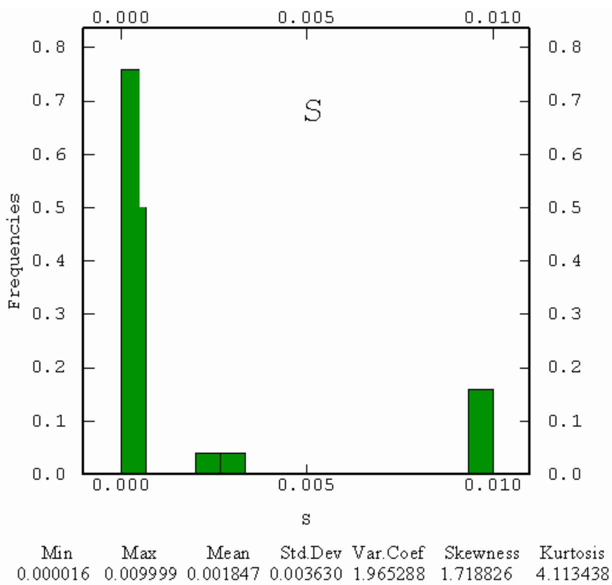

Fig. 4 Histogram of Storage coefficient

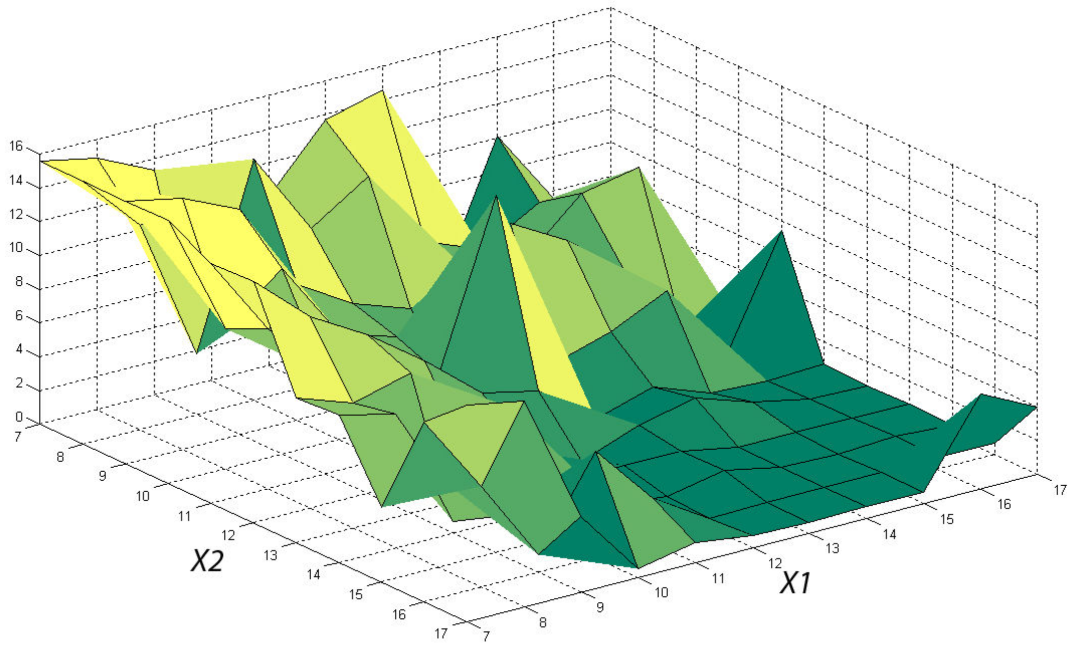

Fig. 5 Validation errors. X1: numbers of nodes of the first hidden layer; X2: numbers of nodes of the second hidden layer

VIII. ANN Training/validation and simulation results

The three-dimensional geo-lithologic model of aquifer is transformed in a 13 input signals for ANN. Each input i^{th} signal represent the density of the correspondent i^{th} lithotype (total volume of lithotype per unit volume of the aquifer). The output of the ANN are 2 signals as: horizontal trasmissivity T and specific storage S previously determinated. In order to have a more efficient training session the input and the output signals are pre-emptively standardized with respect to the range of the all values. In this manner they are scaled in the range [-1, 1]. After training session or simulation the standardized outputs are back-scaled in the original range.

In order to choose various networks models, such as different network architectures, the cross-validation approach called "leave-v-out" are used. The target data set are divided in *k* subsets. In this specific case *k* are set equal to a range of 5 to the total number of targets. The networks are trained *k* times, leaving for each time a subset. When the *k* subsets are terminated, they are used to compute the error of the model through the mean square error approach.

The training/validation session adopts the following algorithm:

1. For each network architecture, for each k value the ANN are trained using Bayesian regularization approaches.
2. Before training a network weight and biases are set to a random value uniformly distributed in the range [-0.15, 0.15];
3. For each iteration step of the training session: Compute the Hessian matrix **A** of the function M(**w**); Set α and β using the following implicit equation [20]:

$$\alpha = \left[n - \alpha \cdot \mathrm{T}\left(\mathrm{A}^{-1}\right)\right] \cdot \left(\sum_{i=1}^{n} w_i^2\right)^{-1}$$

$$\beta = \frac{1}{2}\left[N - n + \alpha \cdot \mathrm{T}\left(\mathrm{A}^{-1}\right)\right] \cdot \left(\sum_{i=1}^{N} e_i^2\right)^{-1};$$

Update weight and biases using Levenberg-Marquardt algorithm. When the training sessions are terminated, compute the validation errors for each k subset.

4. Repeat 2, 3 and 4 steps as long as the validation subsets are terminated.
5. In this way it is possible to choose one or more network architectures that presents the smallest validation error.

This algorithm is performed in scilab environment [21].

The optimal architecture network results constituted by two hidden layers which respectively present 12 and 13 nodes. Fig 5 shows the variation of the validation errors for different architecture models. The correlation coefficient is equal to 0.967 for transmissivity values and 0.996 for storage values.

A qualitative analysis of the maps of Transmissivity (Fig. 6c) and Storage (Fig 6d) obtained reveals interesting results compared with the density maps of silt, clayey silt, silty clay and clay clays (lithotype 9) (Fig 6a) and calcarenitic levels (lithotype 5) (Fig 6b) present in terraced marine deposits.

The comparison shows that in correspondence of zones where the density of lithotype 9 is higher the transmissivity values are lower; as far as lithotype 5, no direct relationship has been detected, as this lithotype can have different degrees of compactness due to different degrees of fracturing or degradation, that provide different transmissivity values. On the other hand, lithotype 5 shows a relationships with the storage coefficient, in fact where the density of lithotype 5 is higher storage values are lower, moreover high density of

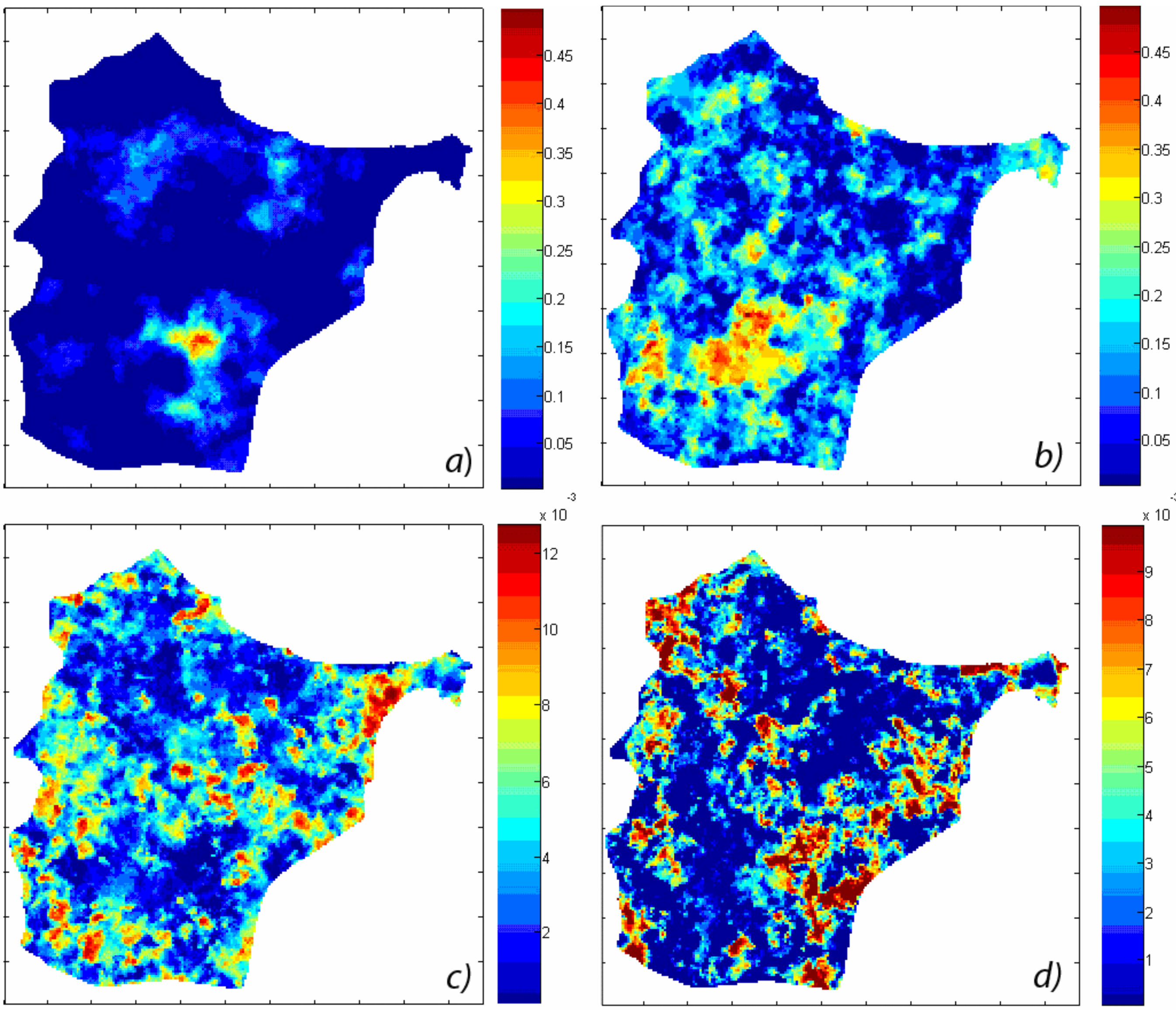

Fig. 6 ANN results. a) density map of silt, clayey silt, silty clay and clay (lithotype 9), b)density map of calcarenitic levels (lithotype 5), c) Transmissivity map [$m^2 \cdot s^{-1}$], d) Storage map [m^{-1}].

lithotype 9 corresponds to high storage values.

These results have proved to be coherent on the hydrogeological and geomechanical point of view. In fact, according with literature [22], values of hydraulic conductivity of silt, clayey silt, silty clay and clay are known to be orders of magnitude lower than K values belonging to calcarenitic levels. As far as storage coefficient, it depends on soil compressibility and porosity; both these parameters are lower for calcarenitic levels compared with silt, clayey silt, silty clay and clay.

A Sequential Gaussian Simulation has been performed on Transmissivity values and the results (Fig 7) have been compared to the ones obtained by means of the integrated approach.

From the comparison it can be emphasized that the simulations obtained by means of the sequential Gaussian method show a more homogeneous behavior than the ones

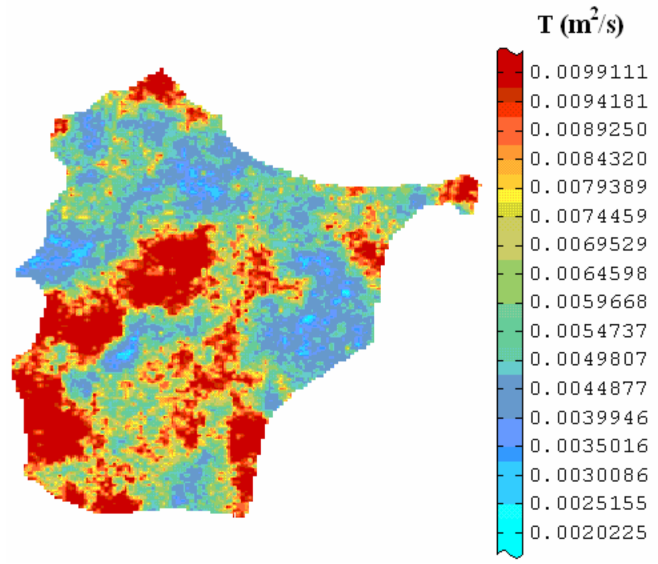

Fig. 7 Sequential Gaussian Simulation of Transmissivity

obtained by considering also the information of the geolithological model. The reason is attributable to the fact that the former is just based on one source of data (Transmissivity values), whereas the latter considers also the conditioning of the geolithology.

IX. Conclusion

This study is aimed at setting up a hydrogeological model of an heterogeneous aquifer by means of an integrated approach.

The geological reconstruction obtained by means of the nested indicator simulation technique has allowed to build an hydrogeological model of the aquifer, by means of conditioning properties such as transmissivity and storage coefficient to the soft information coming from geolithology.

The nested sequential indicator simulation even if remaining a methodology based on two point– statistics has provided a satisfactory detailed geological characterization that coupled with Artificial Neural Networks has allowed to find a relationship between the obtained reconstruction and the in situ measured hydraulic parameters.

The application of the Bayesian regularization and “leave-v-out” cross-validation approach has allowed to choose the optimal regularization parameters and the optimal network architecture. The results obtained have proved to be satisfactory in that the correlation coefficient between target values and simulated values is relatively high. This result is comforted by the qualitative comparison, based on hydrogeological and geomechanical knowledge, between the input density map of lithotypes 9 and 5 and the output maps of the mentioned hydraulic parameters. As far as transmissivity, its values are lower in correspondence of zones where the density of lithotype 9 is higher; whereas, as far as storage coefficient, its values prove to be lower where the density of lithotype 5 is higher, and increase with increasing density of lithotype 9.

The geological and hydrogeological reconstruction obtained by means NSIS and ANN permits to improve the comprehension and to provide an accurate prediction of flow and transport phenomena within the study domain by means of the successive implementation of a numerical modeling. Therefore this knowledge represents an important boundary condition in the economic evaluation connected to resource management, risk assessment and clean up strategies.

References

[1] Castrignanò A., Cherubini Claudia, Giasi C. I., Musci F., Pastore N, Multivariate Geostatistical and Natural Attenuation Model Approach for remediation of chlorinated compounds, WSEAS Transactions On Environment And Development ISSN: 1790-5079 Issue 5, Volume 3, May 2007 [ISI Transaction]

[2] Cherubini Claudia, Concetta I. Giasi, Fausta Musci, Nicola PastorE. (2009). Nested SIS algorithm for a stochastic geolithologic characterization of heterogeneous aquifer. In: Recent Advances in Water Resources, Hydraulics & Hydrology – Mathematics and Computers in Science and Engineering. Published by WSEAS Press, 2009. ISBN: 978-960-474-057-4 ISSN: 1790-2769. (ISI Book).

[3] Ciaranfi N., Pieri P., Ricchetti G., 1992. Note alla carta geologica delle Murge e del Salento (Puglia centromeridionale). Memorie Società Geologica Italiana, 41, 449 – 460.

[4] Journel, A. G., Alabert, F., 1988. Focusing on spatial connectivity of extreme-valued attributes: stochastic indicator models of reservoir heterogeneities, paper SPE 18234.

[5] Gòmez-Hernandez J, 1989. Indicator conditional simulation of the architecture of hydraulic conductivity fields: application to a sand-shale sequence. Groundwater Management: Quantity and Quality (Proceedings of the Benidorm Symposium, October 1989). IAHS Publ. no. 188.

[6] Journel A.G., Gundeso R., Gringarten E., Yao T., 1998. Stochastic modelling of a fluvial reservoir: a comparative review of algorithms. Journal of Petroleum Science and Engineering 21 1998 95–121

[7] Al-Kaabi A. O., Lee W. J., 1990. Using artificial neural network sto identify the well test interpretation model. SPE paper 20332 presented at the Society of Petroleum Engineers Petroleum Computer Conference, Denver, Colorado, June 25-28.

[8] Shimada N., Kozawa T., Yoshioka K., Nishikawa N., Tani A., 1995. Prediction of well-log data by neural network. In Proceedings of the 93rd SEGJ Conference (in Japanese).

[9] Malki H. A., Baldwin J.L., Kwari M. A., 1996. Estimating permeability by use neural network in thinly bedde shaly gas sands. SPE Computer Applications, April 1996.

[10] Yilmaz I., Yuksek A. G., An example of artificial Neural Network (ANN) Application for Indirect Estimation of Rock Parameters. Rock Mechanics and Rock Engineering

[11] Kurtulus B., Razack M., 2007. Evaluation of the ability of an artificial neural network model to simulate the input-output responses of a large karstic aquifer: the La Rochefoucauld aquifer (Charente, France). Hydrogeology Journal 15:241-254.

[12] Lallahem S., Mania J., Hani A., Najjar Y., 2005. On the use of neural networks to evaluate groundwater levels in fractured media. Journal of Hydrology 3007 (2005) 92-111.

[13] Dawson C. W., Wilby R., 1998. An artificial neural network approach to rainfall-runoff modeling. Hydrological Sciences-Journal-des Science Hydrologiques, 43(1)

[14] Zainuddin Z. & Ong P.(2008) Function Approximation Using Artificial Neural Networks WSEAS TRANSACTIONS on MATHEMATICS, Issue 6, Volume 7. ISSN: 1109-2769

[15] Anita S. Gangal, P.K. Kalra, and D.S.Chauhan (2009) Inversion of Complex Valued Neural Networks Using Complex Back-propagation Algorithm INTERNATIONAL JOURNAL OF MATHEMATICS AND COMPUTERS IN SIMULATION Issue 1, Volume 3

[16] Lampton, M. Damping-undamping Strategies for the Levenberg-Marquardt Nonlinear Least Square Method. Computers in Physics, Vol. 11, No 1, Jan/Feb 1997. Pp 110-115

[17] MacKay D.j.C. 1992 Bayesian interpolation. Neural Computation, 4(3), 415-47.

[18] MacKay D.J.C, Takeuchi R. 1998. Interpolation models with multiple hyperparameters. Statistics and Computing 8, 15-23.

[19] E. Custodio, M.R.Llamas , *Hydrologia subterranea* , 2 vol., Omega, Barcellona, 1983

[20] MacKay D.J.C.. 1995. Probable networks and plausible predictions—a review of practical Bayesian methods for supervised neural networks. Network: Computation in Neural Systems Vol. 6, No. 3, pp. 469–505.

[21] Scilab 5.11 Consortium/INRIA/ENPC/Contributors.

[22] Domenico P.A. & Schwartz F.W. (1990) Physical and Chemical Hydrogeology. John Whiley & Sons, Inc., New York

Claudia Cherubini Graduated cum laude in 2003, PhD since 2007, currently Post Doc Scholarship at Polytechnic of Bari. Visiting Researcher in 2006 at Lawrence Berkeley National Laboratory (LBNL) and in 2005 at Geowissenschaftliches Zentrum der Universität Göttingen. Specific roles in important International Research Projects among which: Yucca Mountain Project of LBNL; European Research Project “KORA” of Universität Göttingen. European Project PRIMAC “Protection of coastal aquifers from seawater intrusion”. Member of different International Scientific Committees of International Congresses, inserted in some International Program Committees, invited to be Rewiever and Speaker in the International Congresses. In 2008 didactic activity within the course “PhD International

course on Advanced numerical modeling of flow and transport in soils and aquifers (ANMFT)", at University of Siena. Winner of international Prize "Best Student Paper" for the scientific paper "A hydrodynamic model of a contaminated fractured aquifer" presented at the Int. Conf. 5th IASME / WSEAS 2007. Only Italian Winner of an international selection of 35 experts in 2003. Winner of a Post doctorate Research Scholarship at University of Sannio; holder of a Post doctorate Research Scholarship at CNR. Attendance of several international training Courses. More than 40 papers published on Scientific Journals, International Books and Conference Proceedings and n. 2 final reports of European Research Projects. Some papers subject of international Selection. Certified knowledge of 6 foreign languages: English, German, Spanish, French, Portuguese and Japanese.

Fausta Musci PhD student of the "Scuola Interpolitecnica di Dottorato" (SIPD) – Area ETSC (Environmental and Territorial Safety and Control) in "Engineering and Chemistry for the safeguard of the ecosystems" Polytechnic of Bari department of Water Engineering and Chemistry. Graduated cum laude in March 2007 at First Faculty of Environmental Engineering (Polytechinc of Bari). Currently, in research period at Centre de Geosciences – Ecoles de Mines de Paris. Attendance of international course: Advanced Numerical Modeling Of Flow And Transport In Soils And Aquifers, Università degli studi di Siena, Attendance of International course "Les Méthodes de la Géostatistique: Géostatistique non-stationnaire et multivariable, Géostatistique non-linéaire et simulations", c/o Centre de Geosciences – Ecole des Mines de Paris. Attendance of the course "Simulations", part of the "**C**ycle de **F**ormation **S**pécialisée en **G**éostatistique" c/o Ecole des Mines de Paris. Research activity developed at the department of Civil and Environmental Engineering of the Polytechnic of Bari on: Geostatistical techniques applied to the hydrogeology, Geolithological and hydrogeological characterization of reservoir based on (non)linear and (non)parametric geostatistical techniques. Collaboration contract with Polytechnic of Bari Department of Civil and Environmental Engineering, about groundwater modeling on the area of Salento peninsula (Italy).

Nicola Pastore PhD student in "Engineering and Chemistry for the safeguard of the ecosystems" Polytechnic of Bari department of Water Engineering and Chemistry. Graduated in 2007 at First Faculty of Civil Engineering (Polytechinc of Bari). Attendance of international course: Advanced Numerical Modeling Of Flow And Transport In Soils And Aquifers, Università degli studi di Siena. Collaboration contract with SISTEMI INDUSTRIALI S.r.l. C.da S. Cusumano 96011 Augusta (SR) (Italy), the activities focuses on development a new groundwater cleanup technique by numerical simulation. Collaboration contract with Polytechnic of Bari Department of Civil and Environmental Engineering, about groundwater modeling on the area of Salento peninsula (Italy). Lecturer at workshop on: "Modelli di flusso nelle rocce fratturate e carsiche" October 2008, Brindisi; "Inquinamento Ambientale e Bonifiche" Tecnologie e servizi innovativi per la gestione e prevenzione dei rischi naturali ed antropici ImpresAmbiente, Potenza. December 2008.

Research activity developed at the department of Civil and Environmental Engineering of the Polytechnic of Bari on: Modeling multiphase flow and reactive multi component transport in fractured karstic reservoir; Development of algorithms for inverse modeling problem based on fuzzy logic and global optimization techniques; Geolithological and hydrogeological characterization of reservoir based on (non)linear and (non)parametric geostatistical techniques; modeling seawater intrusion and development of remediation strategies.